Deletion of the Androgen Receptor in Adipose Tissue in Male Mice Elevates Retinol Binding Protein 4 and Reveals Independent Effects on Visceral Fat Mass and on Glucose Homeostasis

Kerry J. McInnes,[1] Lee B. Smith,[2] Nicole I. Hunger,[1] Philippa T.K. Saunders,[2] Ruth Andrew,[1] and Brian R. Walker[1]

Testosterone deficiency is epidemic in obese ageing males with type 2 diabetes, but the direction of causality remains unclear. Testosterone-deficient males and global androgen receptor (AR) knockout mice are insulin resistant with increased fat, but it is unclear whether AR signaling in adipose tissue mediates body fat redistribution and alters glucose homoeostasis. To investigate this, mice with selective knockdown of AR in adipocytes (fARKO) were generated. Male fARKO mice on normal diet had reduced perigonadal fat but were hyperinsulinemic and by age 12 months, were insulin deficient in the absence of obesity. On high-fat diet, fARKO mice had impaired compensatory insulin secretion and hyperglycemia, with increased susceptibility to visceral obesity. Adipokine screening in fARKO mice revealed a selective increase in plasma and intra-adipose retinol binding protein 4 (RBP4) that preceded obesity. AR activation in murine 3T3 adipocytes downregulated RBP4 mRNA. We conclude that AR signaling in adipocytes not only protects against high-fat diet–induced visceral obesity but also regulates insulin action and glucose homeostasis, independently of adiposity. Androgen deficiency in adipocytes in mice resembles human type 2 diabetes, with early insulin resistance and evolving insulin deficiency. ***Diabetes*** **61:1072–1081, 2012**

Testosterone deficiency is being diagnosed with increasing frequency in older men with obesity and type 2 diabetes. Although obesity may be a reversible risk factor for low testosterone levels, an increasing body of evidence suggests that low testosterone promotes insulin resistance and increases the risk of type 2 diabetes (1–3). Furthermore, testosterone replacement therapy improves glycemic control in hypogonadal men with type 2 diabetes (4). However, the amount and distribution of body fat is also strongly influenced by sex steroids, and low plasma testosterone levels are associated with visceral obesity (5,6), an independent risk factor for insulin resistance and type 2 diabetes. It is unclear whether testosterone deficiency directly promotes insulin resistance and hyperglycemia over and above its association with visceral obesity.

Testosterone exerts its effects by binding to the androgen receptor (AR), which mediates most of its biological functions through transcriptional activation of downstream genes. ARs are present in adipose tissue, at a higher level in visceral fat than other adipose depots (7), and AR activation affects adipocyte differentiation (8) and lipid metabolism (9). However, although global deletion of AR in mice results in late-onset obesity (10) accompanied by adipocyte hypertrophy (11), adipocyte-specific AR knockdown (crossing aP2-*cre* with floxed AR mice) had no reported effect on body weight, adiposity, or fasting plasma glucose and insulin concentrations, despite reducing plasma lipids (12). This contrasts with increased susceptibility to obesity, hepatic steatosis, hyperinsulinemia, and hyperglycemia in mice with liver-specific AR deletion (13). However, since the adipose-specific AR knockdown mice were studied only by fasting blood samples at age 20 weeks and without high-fat (HF) diet, and given that androgen deficiency predisposes to age-associated deterioration in glucose homoeostasis, we speculated that a more subtle phenotype might result from androgen deficiency in adipose tissue and that effects on fat redistribution/accumulation may be separable from those on insulin sensitivity and glucose homoeostasis.

RESEARCH DESIGN AND METHODS

Breeding and maintenance of transgenic mice. Male mice in which AR has been selectively knocked down in adipose tissue were generated using *Cre/loxP* technology. Male mice heterozygous for *Cre* recombinase under the control of the fatty acid binding protein aP2 promoter (The Jackson Laboratories) or the adiponectin promoter (14), both on a C57Bl/6 congenic background, were mated to female mice homozygous for a floxed AR on the X chromosome, also on a C57Bl/6 background (15). The aP2-*Cre*-positive, AR^{flox}-positive male offspring from these matings are termed fARKO, and the adiponectin-*Cre*-positive, AR^{flox}-positive male offspring are termed adipoQ-fARKO. The *Cre*-negative, AR^{flox}-positive littermates were used as controls (termed control). Sex and genotype ratios were all produced at the expected Mendelian ratios. All mice were bred under standard conditions of care and used under licensed approval from the U.K. Home Office. Animals were fed standard chow (product 801151; Special Diet Services, Essex, U.K.) ad libitum unless stated otherwise. Genotyping was performed using genomic DNA isolated from the ear for the presence of *Cre* by PCR (http://jaxmice.jax.org/protocolsdb/f?p=116:2:3835741438358292::NO:2:P2_MASTER_PROTOCOL_ID,P2_JRS_CODE:288%2C005069).

Females homozygous for AR^{flox} were identified using primers for AR exon 2. All fARKO male offspring were genotyped for the presence of *Cre* using the primers detailed above. The assessment of AR recombination was performed by RT-PCR from cDNA from isolated tissues from fARKO and adipoQ-fARKO mice and control littermates using a previously described PCR strategy (16) in which a 765–base pair amplified product indicated mice with a floxed allele of AR and a 613–base pair product indicated mice with an excised exon 2 allele of AR.

From the [1]Endocrinology Unit, University/British Heart Foundation Centre for Cardiovascular Science, University of Edinburgh, Queen's Medical Research Institute, Edinburgh, Scotland, U.K.; and the [2]Medical Research Council Centre for Reproductive Health, University of Edinburgh, Queen's Medical Research Institute, Edinburgh, Scotland, U.K.
Corresponding author: Kerry J. McInnes, kerry.mcinnes@ed.ac.uk.
Received 17 August 2011 and accepted 26 January 2012.
DOI: 10.2337/db11-1136
This article contains Supplementary Data online at http://diabetes.diabetesjournals.org/lookup/suppl/doi:10.2337/db11-1136/-/DC1.

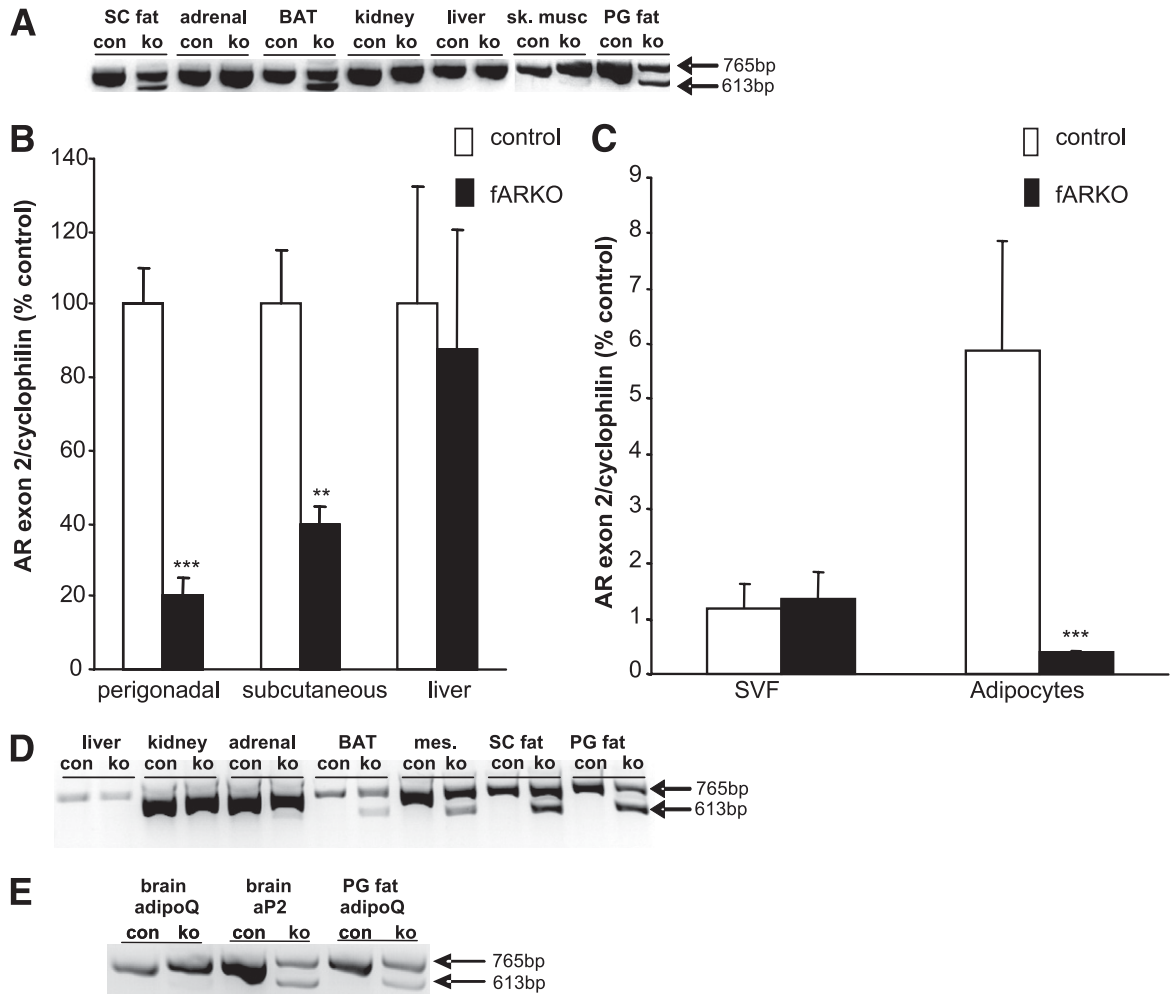

FIG. 1. Generation of male fat-specific AR knockouts. *A*: Deletion of AR in the fat was determined using RT-PCR spanning exon 2. Only the larger 765bp floxed band was seen in adrenal, kidney, skeletal muscle (sk.musc), and liver. Both bands were identified in subcutaneous (SC) and perigonadal (PG) fat and in brown adipose tissue (BAT) showing deletion of the AR in a proportion of cells in white and brown adipose tissue. *B*: Quantitative real-time PCR using AR exon 2-specific primers confirmed loss of AR exon 2 in subcutaneous and gonadal fat, but not in the liver of fARKO mice. *C*: Quantitative real-time PCR using AR exon 2-specific primers confirmed loss of AR exon 2 in the adipocyte fraction only of gonadal fat. *D*: Deletion of AR in the fat of adipoQ-fARKO mice was determined using RT-PCR spanning exon 2. Only the larger 765bp floxed band was seen in adrenal, kidney, and liver. Both bands were identified in SC fat, PG fat, mesenteric (mes.) fat, and in BAT showing deletion of AR in a proportion of cells in white and brown adipose tissue. *E*: Deletion of AR exon 2 was determined in the brain using RT-PCR. AR exon 2 was deleted in the brain of fARKO mice generated with aP2-*Cre* (aP2) but not in mice using adiponectin-*Cre* (adipoQ). Data are mean ± SEM (n = 8–10). **P < 0.01 control vs. fARKO; ***P < 0.001 control vs. fARKO. bp, base pair; con, control; ko, knockout.

Experimental design. Male mice maintained on standard chow diet (n = 8–10 per group) were killed at various postnatal ages (3, 6, and 12 months) by inhalation of CO_2 and subsequent cervical dislocation. Immediately after killing, blood was collected from mice by cardiac puncture. Plasma was separated and stored at −20°C until assayed. Body weight was measured and liver and adipose tissue beds (perigonadal, subcutaneous, mesenteric, omental, and interscapular brown) were removed and weighed. Tissues were either snap frozen for subsequent RNA and protein analysis or fixed in Bouin fixative for 6 h. A further cohort of male fARKO and control mice (n = 8–10 per group) were maintained on standard chow, and intraperitoneal glucose tolerance tests (GTTs) were performed after a 6-h fast at age 3, 6, 9, and 12 months as previously described (17). For insulin signaling experiments, a further cohort of 3-month-old male mice (n = 6 per group) were fasted for 6 h, injected with insulin (10 mU/g body wt i.p.), and killed 10 min later. Perigonadal and subcutaneous adipose tissue was dissected and snap frozen in liquid N_2.

To address responses to a diet previously optimized for inducing weight gain and insulin resistance (18), groups of male fARKO and control mice (n = 8–10 per group) were fed an HF diet (product D12331, 58% calories as fat with sucrose; Research Diets, New Brunswick, NJ) for a period of 24 weeks. After 6, 12, and 24 weeks of HF-diet feeding, body weight was measured and intraperitoneal GTTs were performed as described above. Mice were killed after 24 weeks of HF diet. Plasma was prepared as described above, and liver and adipose tissue beds were dissected, weighed, and snap frozen for subsequent analysis.

Biochemical assays. Testosterone was measured using a previously published radioimmunoassay (19). All samples from each mouse were run in a single assay, and the within-assay coefficients of variation were all <10%. Glucose was determined by the hexokinase method (Sigma-Aldrich, Dorset, U.K.) and plasma insulin and leptin by ELISA (Crystal Chem, Inc., Downers Grove, IL). On a subset of animals, triglycerides and total cholesterol were measured in fasting plasma by colorimetric enzyme assay (Thermo Electron, Melbourne, Australia). Nonesterified fatty acid (NEFA) levels were analyzed using a NEFA-kit (Wako Chemicals GmBH).

Hepatic triglyceride content. Liver was homogenized in 4–10 vol propan-2-ol (VWR International Ltd., Lutterworth, U.K.) for 2 × 20 s and cleared of debris by centrifugation (>10,000*g* for 10 min), and the supernatant was assayed using a triglyceride kit (Thermo Electron).

Plasma retinol binding protein 4 measurement. Plasma was diluted 10 times in sample buffer (0.125 mol/L Tris pH 6.8, 4% SDS, 20% glycerol, 0.2 mg/mL bromophenol blue) containing dithiothreitol (200 mmol/L), and proteins were separated by 15% SDS-PAGE and transferred to nitrocellulose membranes. Mouse retinol binding protein 4 (RBP4) was detected using anti-human RBP4 polyclonal antisera (DAKO) (20). The anti-human antibody also recognizes mouse RBP4 but with lower affinity.

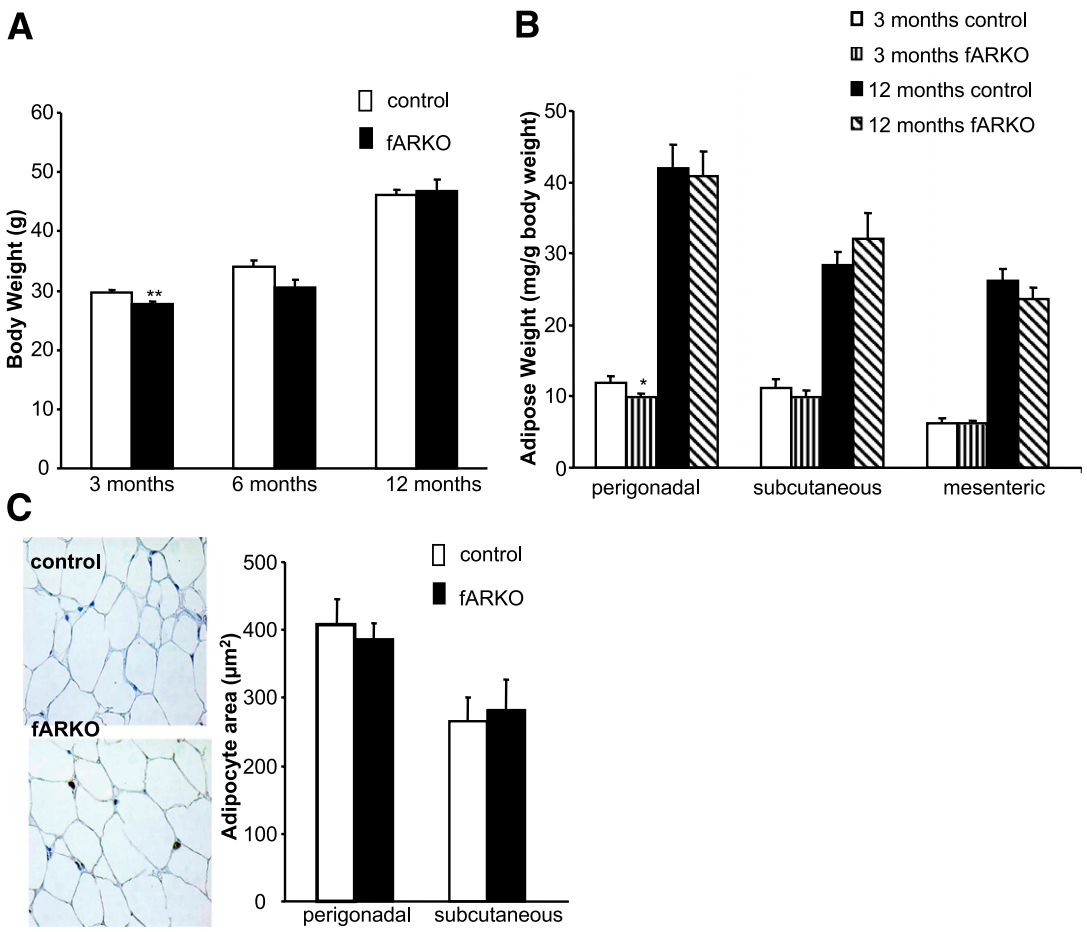

FIG. 2. Body and fat pad weights on normal chow diet. *A*: Body weight of male fARKO and control mice on standard chow and aged 3, 6, and 12 months. *B*: Relative fat pad masses of male fARKO and control mice on standard chow and aged 3 and 12 months. Data are mean ± SEM (n = 8–10). *P < 0.05, **P < 0.01 control vs. fARKO. *C*: There was no difference between fARKO and control mice on standard chow and aged 3 months in the morphology or size of white adipose tissue from the perigonadal or subcutaneous fat pad. Data are representative images from the two experimental groups (n = 3). (A high-quality color representation of this figure is available in the online issue.)

White adipose tissue histology. Bouin-fixed perigonadal fat pads were processed and embedded in paraffin wax, and 5-μm sections were stained with hematoxylin-eosin. Images were acquired using a Zeiss microscope (Welwyn Garden City, Hertfordshire, U.K.) equipped with a Kodak DCS330 camera (Eastman Kodak, Rochester, NY).

Adipocyte size. Adipocyte size was determined by measuring adipocytes from 20 randomly selected areas in sections from perigonadal and subcutaneous fat depots of 3-month-old fARKO and control mice fed a normal chow diet using a Zeiss KS300 image analyzer. The marker was blind to genotype.

Adipocyte and stromal vascular fraction isolation. The adipocyte and stromal vascular fraction (SVF) were isolated from perigonadal fat pads as described previously (21). In brief, fat pads were chopped with fine scissors and digested with 2 mg/mL collagenase type 1 (Worthington Biochemical, Reading, U.K.) in Hanks' buffered saline solution (Life Technologies, Inc., Paisley, Scotland) for 1 h at 37°C, then washed twice with Hanks' buffered saline solution. Digested material was separated by centrifugation at 1,000*g* for 8 min (Heraeus; DJB Labcare, Buckinghamshire, U.K.). Freshly isolated SVF fraction and cell supernatant (adipocyte fraction) were then added to TRIzol (Invitrogen, Paisley, Scotland) for RNA extraction.

Quantitative analysis of mRNA. Total RNA was extracted from snap-frozen tissue samples or adipocyte fractions using TRIzol reagent (Invitrogen) and the RNeasy Mini system (QIAGEN, Crawley, U.K.). RNA was reverse transcribed using the Quantitect reverse-transcription kit (QIAGEN). cDNA (equivalent to 250 ng total RNA) was incubated in triplicate with gene-specific primers (Invitrogen) and fluorescent probes (using the Universal Probe Library system [Roche Applied Science, Burgess Hill, U.K.]) in 1× Roche LightCycler 480 Probes mastermix (Supplementary Table 1). PCR cycling and detection of fluorescent signal was carried out using a Roche LightCycler 480. A standard curve was constructed for each primer-probe set using a serial dilution of cDNA pooled from all samples. Results were corrected for the expression of β-actin, which did not change between groups.

Western blotting to investigate signal transduction. Lysates were prepared from perigonadal and subcutaneous fat by extraction in ice-cold buffer as described above. Adipose tissue lysates (500 μg) were subjected to immunoprecipitation with anti-insulin receptor substrate (IRS)1 (4 μg) antibody (Millipore, Watford, U.K.). Immune complexes were collected on protein A-Sepharose beads (Pierce), washed three times with lysis buffer and twice with 1× PBS containing 2 mmol/L Na_3VO_4, resuspended in SDS-PAGE sample buffer, and heated for 10 min at 95°C. Western blotting was performed using phosphospecific antibodies to IRS-1 Tyr-612 (Invitrogen). Proteins were visualized with an Alexa Fluor 800 goat anti-rabbit secondary antibody (LI-COR Biosciences, Lincoln, NE), and band intensities were quantified using the Odyssey infrared imaging system (LI-COR Biosciences).

Adipocyte cell culture. 3T3-L1 cells were seeded at 3×10^5/mL in six-well plates and maintained at no higher than 70% confluence in Dulbecco's modified Eagle's medium supplemented with 10% FCS, 100 IU/mL penicillin, 100 μg/mL streptomycin, and 200 mmol/L L-glutamine (all from Lonza Biologics, Tewkesbury, U.K.). Differentiation of cells into mature adipocytes was induced as previously described (22). Medium was replaced with serum- and phenol red–free Dulbecco's modified Eagle's medium for 24 h before treatment with dihydrotestosterone (DHT; Sigma-Aldrich) at 100 nmol/L for 24 h. After treatment with DHT, cells were washed with ice-cold PBS and lysed in ice-cold buffer (5 mmol/L HEPES, 137 mmol/L NaCl, 1 mmol/L $MgCl_2$, 1 mmol/L $CaCl_2$, 10 mmol/L NaF, 2 mmol/L EDTA, 10 mmol/L Na pyrophosphate, 2 mmol/L Na_3VO_4, 1% Nonidet P-40, and 10% glycerol) containing protease inhibitors (Complete Mini; Roche Diagnostics Ltd.) as previously described (22). Cell lysate (50 μg) was subjected to SDS-PAGE, and RBP4 levels were assayed by Western blotting with an RBP4 antibody as described above. Proteins were visualized and quantified as described above.

Statistical analysis. Data are expressed as means ± SE. Data were analyzed using GraphPad Prism (version 4; GraphPad Software Inc., San Diego, CA) using two-tailed unpaired Student *t* tests.

RESULTS

Generation of mice with fat-specific deletion of ARs. In male fARKO mice, AR expression was preserved in adrenal, kidney, liver, and skeletal muscle (Fig. 1*A*). Brown and white adipose tissue from fARKO mice expressed both the floxed and knockout mRNA band, demonstrating that AR had been deleted from a proportion of cells within the adipose tissue (Fig. 1*A*). AR mRNA was reduced by 70–80% in whole adipose tissue (Fig. 1*B*) and by 85–95% in isolated adipocytes of fARKO mice (Fig. 1*C*). The remaining AR expression could be derived from vascular endothelial cells or stromal cells since AR exon 2 expression was preserved in the SVF (Fig. 1*C*). It is important that circulating testosterone levels were not different between control and fARKO littermates (3 months: 2.0 ± 1.34 vs. 2.3 ± 1.7 ng/mL; 12 months: 2.36 ± 0.78 vs. 2.01 ± 0.97 ng/mL, respectively).

Since AP2-*Cre* is known to be expressed also in the central nervous system (CNS), and fARKO mice showed AR deletion in CNS as well as adipose tissue (Fig. 1*E*), adipoQ-fARKO mice were also generated. AdipoQ-fARKO mice exhibit AR deletion in all adipose depots (Fig. 1*D*) but not in CNS (Fig. 1*E*).

fARKO mice have impaired insulin sensitivity and age-related glucose intolerance, independently of obesity. Age-dependent differences in body composition and glucose/insulin homoeostasis in male mice on normal chow diet are shown in Figs. 2 and 3. At age 3 months, fARKO mice had gained less weight than controls (Fig. 2*A*), with perigonadal fat reduced in weight (0.27 ± 0.017 vs. 0.36 ± 0.02 g, $P < 0.01$) and proportion (Fig. 2*B*), while

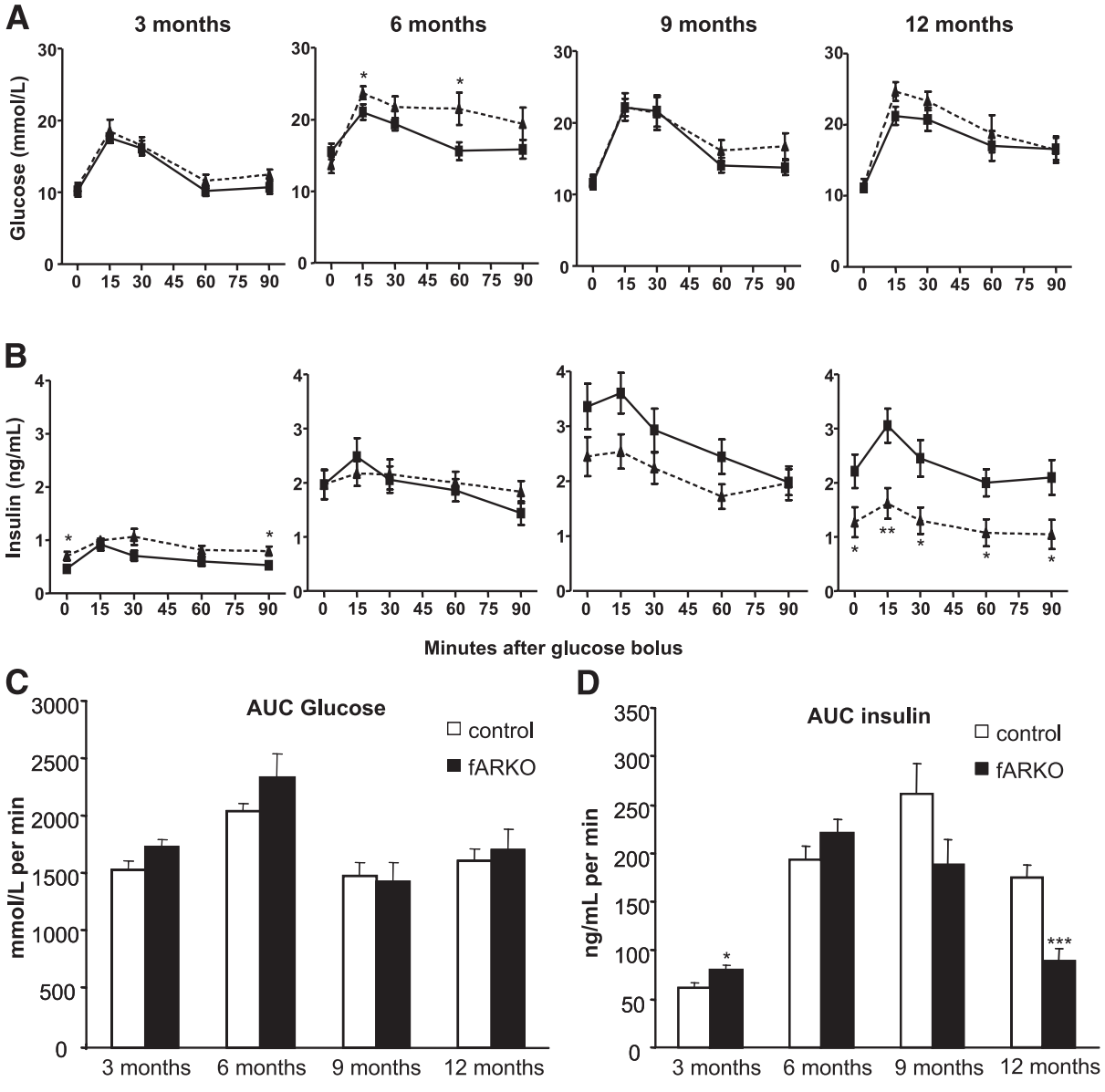

FIG. 3. Glucose homeostasis on normal chow diet. Plasma glucose (*A* and *C*) and plasma insulin (*B* and *D*) during intraperitoneal GTT of male control and fARKO mice on standard chow at 3, 6, 9, and 12 months of age. Mice were fasted for 6 h before testing. Solid line denotes control mice; broken line denotes fARKO mice. Area under the curve (AUC) for all groups shown for glucose (*C*) and insulin (*D*). Data are mean ± SEM (n = 8–10) for individual time points. *$P < 0.05$, **$P < 0.01$, ***$P < 0.001$ control vs. fARKO.

TABLE 1
Metabolic parameters for fARKO mice

	Control	fARKO
Liver triglycerides (μmol/g)	11.3 ± 0.4	11.8 ± 0.4
Plasma triglycerides (mmol/L)	0.6 ± 0.03	0.95 ± 0.09*
Plasma NEFA (mmol/L)	0.77 ± 0.03	0.84 ± 0.06
NEFA suppression (%)	19.2 ± 3.4	15.2 ± 3.3
Plasma total cholesterol (mmol/L)	1.88 ± 0.2	1.65 ± 0.1

Data are mean ± SEM (n = 8–10). Liver and plasma triglycerides, NEFAs, and total cholesterol levels were analyzed in 3-month-old fARKO and control littermates maintained on standard chow diet. Plasma triglycerides, NEFAs, and total cholesterol were measured in fasted (6 h) animals. Liver triglycerides were measured in fed animals. NEFA suppression was calculated as the percent suppression in plasma NEFA levels measured between 0 and 15 min after a glucose bolus was administered to 6-h–fasted animals. *$P < 0.05$ vs. control.

only interscapular brown adipose tissue was proportionately increased in 3-month-old fARKO males (5.0 ± 0.3 vs. 4.1 ± 0.3 mg/g, $P = 0.02$). White adipose tissue morphology and adipocyte size in the perigonadal and subcutaneous depots were unaltered (Fig. 2*C*). Body composition was no longer significantly different by age 6 months and remained similar at age 12 months (Fig. 2*A* and *B*).

Despite their lack of obesity at age 3 months, fARKO mice were euglycemic (Fig. 3*A* and *C*) but hyperinsulinemic (Fig. 3*B* and *D*) both in the fasted state and during GTT. At age 3 months, fARKO mice had normal liver triglycerides but elevated plasma triglyceride levels (Table 1). Although plasma NEFA levels and the suppression rate of NEFA in response to a glucose bolus were not significantly different between the groups (Table 1), transcript levels for hormone-sensitive lipase and lipoprotein lipase were elevated in perigonadal and subcutaneous adipose tissue, and transcript levels for adipose triglyceride lipase and fatty acid synthase were elevated specifically in subcutaneous adipose tissue (Fig. 4*A*). Adipose insulin resistance was confirmed in fARKO mice at age 3 months, since in perigonadal and subcutaneous adipose tissue, total IRS-1 levels were comparable to those seen in wild-type mice,

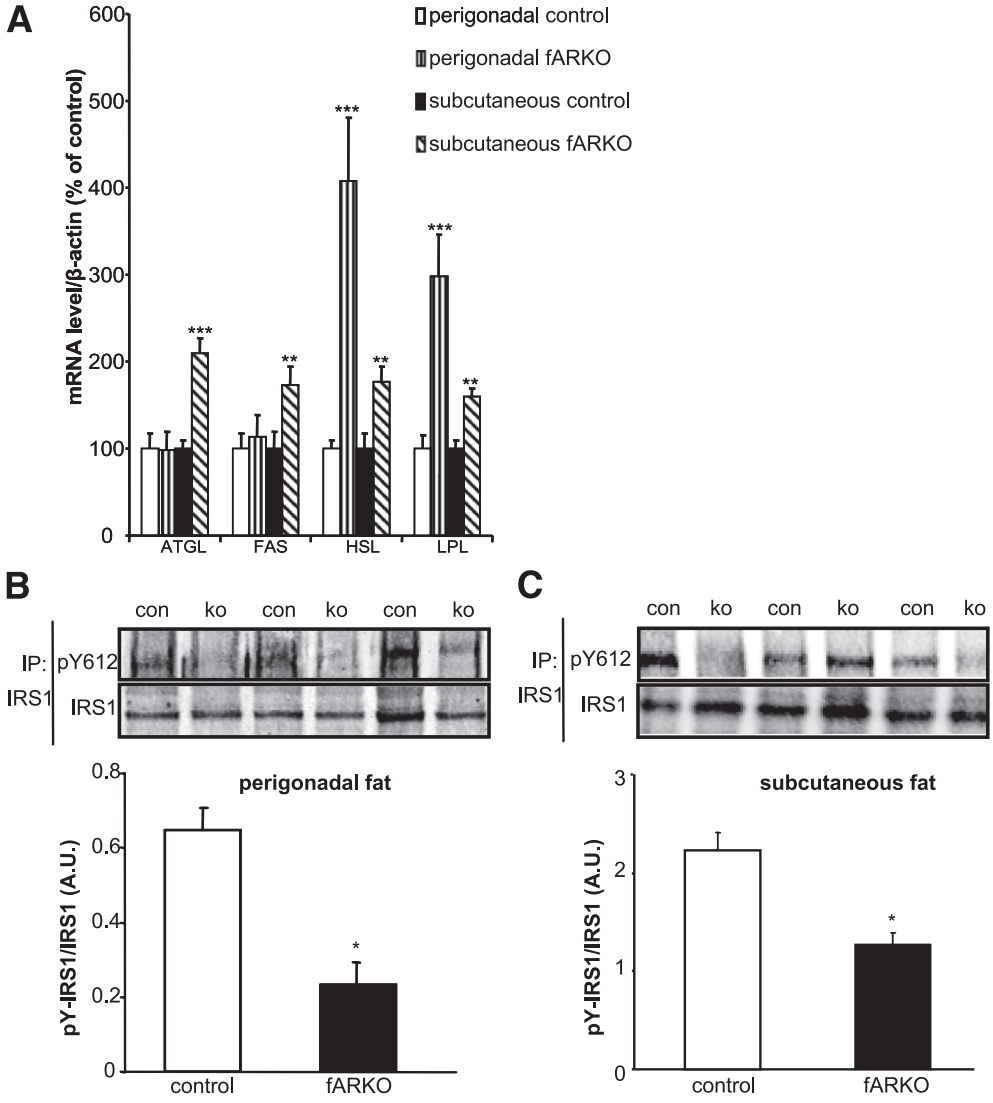

FIG. 4. Adipose transcript levels and adipose insulin resistance in fARKO mice. *A*: mRNA levels were measured for adipose triglyceride lipase (ATGL), fatty acid synthase (FAS), hormone-sensitive lipase (HSL), and lipoprotein lipase (LPL) by quantitative PCR in perigonadal and subcutaneous adipose tissue of 3-month-old fARKO and control mice on standard chow. *B* and *C*: Representative Western blots of IRS-1 pY612 phosphorylation in perigonadal and subcutaneous adipose tissue lysates. Data are mean ± SEM; (n = 8–10). *$P < 0.05$ control vs. fARKO, **$P < 0.01$ control vs. fARKO, ***$P < 0.001$ control vs. fARKO. con, control; ko, knockout; IP, immunoprecipitation; A.U., arbitrary unit.

but insulin-stimulated IRS-1 Tyr phosphorylation was reduced (Fig. 4*B* and *C*).

Between age 3 and 12 months, fARKO mice were unable to sustain the normal increase in insulin secretory capacity, and they developed hyperglycemia. As a result, at age 6 months, when fARKO mice were in transition between hyperinsulinemia and insulin deficiency, there were no statistically significant differences in glucose and insulin levels either fasted or during a GTT (Fig. 3*A* and *B*).

fARKO mice are more susceptible to HF diet–induced visceral obesity and glucose intolerance. With HF feeding, AR expression in adipose tissue was reduced to a similar level as seen with normal diet; no evidence of extra-adipose *Cre* expression was observed, and circulating testosterone levels were unaffected by diet or AR knockdown (2.9 ± 0.5 vs. 4.4 ± 3.2 ng/mL in fARKO and controls, respectively, after 24 weeks). On HF diet, male fARKO mice gained equal weight compared with controls (Fig. 5*A*) but, after 24 weeks, had more visceral fat, with increased omental and mesenteric fat pad weights (Fig. 5*B*). Control animals on HF diet were hyperglycemic after 6 weeks but showed a progressive increase in insulin secretion such that glucose tolerance, if anything, improved by 24 weeks (Fig. 6). In contrast, fARKO mice had a poorer insulin secretory response and became significantly more hyperglycemic than control mice at 24 weeks (Fig. 6). There was no increase in triglyceride accumulation in the livers (0.05 ± 0.01 vs. 0.05 ± 0.007 mmol/L) or plasma (1.03 ± 0.07 vs. 0.93 ± 0.08 mmol/L) of fARKO mice compared with controls, and plasma NEFA levels were not different between groups after 24 weeks on HF diet (0.61 ± 0.04 vs. 0.73 ± 0.09 mmol/L in fARKO and controls, respectively).

Impaired insulin sensitivity in fARKO mice is associated with an altered adipokine profile and AR-dependent increased RBP4 levels. To identify adipose-derived factors that might mediate insulin resistance in the absence of obesity, we focused on samples from 3-month-old male mice on normal chow diet. Contrary to a previous report of similar 20-week-old animals (12), neither leptin transcript levels in adipose depots (Fig. 7*A*) nor fasted or fed plasma leptin levels differed between fARKO and control mice (Fig. 7*B*). Adiponectin transcript levels were elevated, rather than downregulated, in perigonadal and subcutaneous fat of fARKO mice (Fig. 7*A*). Resistin mRNA was modestly increased selectively in subcutaneous fat in fARKO mice (Fig. 7*A*). However, RBP4 mRNA in both perigonadal and subcutaneous adipose (Fig. 7*A*) and protein levels in plasma (Fig. 7*C*) were increased in fARKO mice with no difference in hepatic RBP4 transcript levels (Fig. 7*D*). This adipose-specific AR-mediated regulation of RBP4 was further confirmed in a second fat-specific ARKO model driven by the adiponectin promoter (Fig. 7*E*).

In differentiated 3T3-L1 adipocytes, the nonaromatizable androgen DHT reduced RBP4 mRNA levels (Fig. 7*F*).

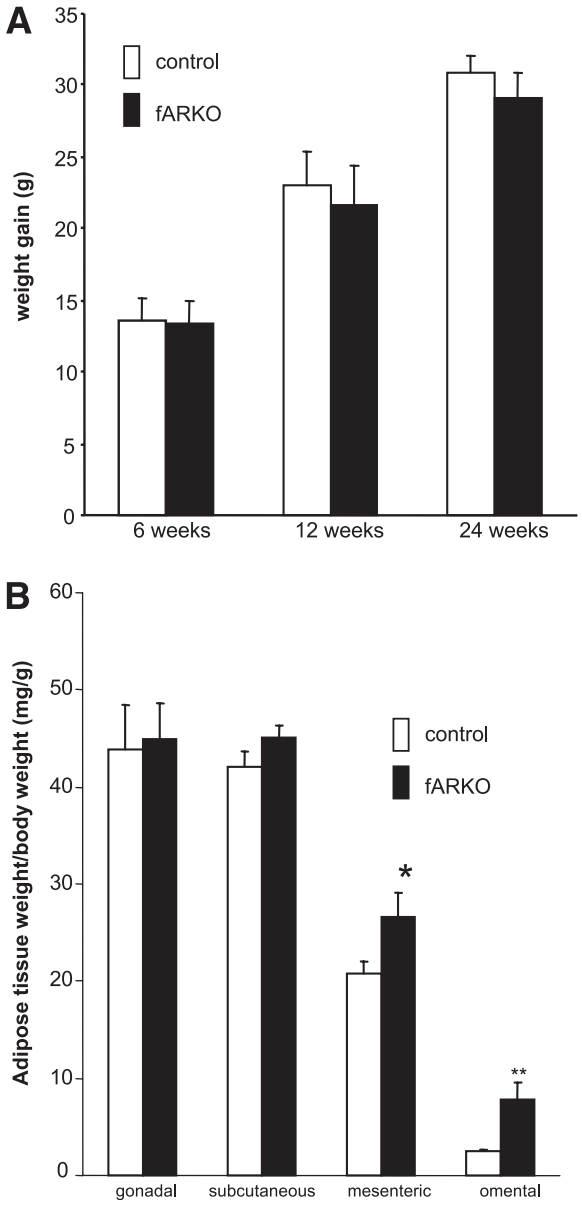

FIG. 5. Effect of HF diet on body composition. *A*: Weight gain after 6, 12, and 24 weeks of HF diet. *B*: Relative fat pad masses of male fARKO and control mice fed an HF diet for 24 weeks. Data are mean ± SEM (n = 8–10). *P < 0.05, **P < 0.01 control vs. fARKO.

DISCUSSION

We have demonstrated an important role for AR in adipose tissue in regulating glucose/insulin homeostasis in mice. Male fARKO mice exhibit a pattern of age-dependent metabolic dysregulation typical of the evolution of human type 2 diabetes, with early insulin resistance/hyperinsulinemia/hypertriglyceridemia followed by later insulin deficiency on normal chow and accelerated insulin deficiency and hyperglycemia on HF diet. This dynamic evolution likely explains the absence of a detectable metabolic phenotype in previous studies of a similar strain of mice at age 5 months (12). Furthermore, although fARKO mice are more susceptible to visceral obesity on HF diet, obesity is not a prerequisite for early insulin resistance or later insulin deficiency in these mice; indeed, at age 3 months, insulin resistant fARKO mice are smaller with less body fat than controls. Unlike liver-specific AR-deficient mice (13), there was no evidence of hepatic steatosis and normal NEFA levels in fARKO mice, making "spillover" of fatty acids into extra-adipose organs unlikely as a mechanism underlying their insulin resistance. However, consistent with adipose tissue–dependent insulin resistance without obesity, fARKO mice showed an unusual pattern of altered adipokines, with paradoxically elevated adiponectin, normal leptin, and elevated RBP4. The inferred

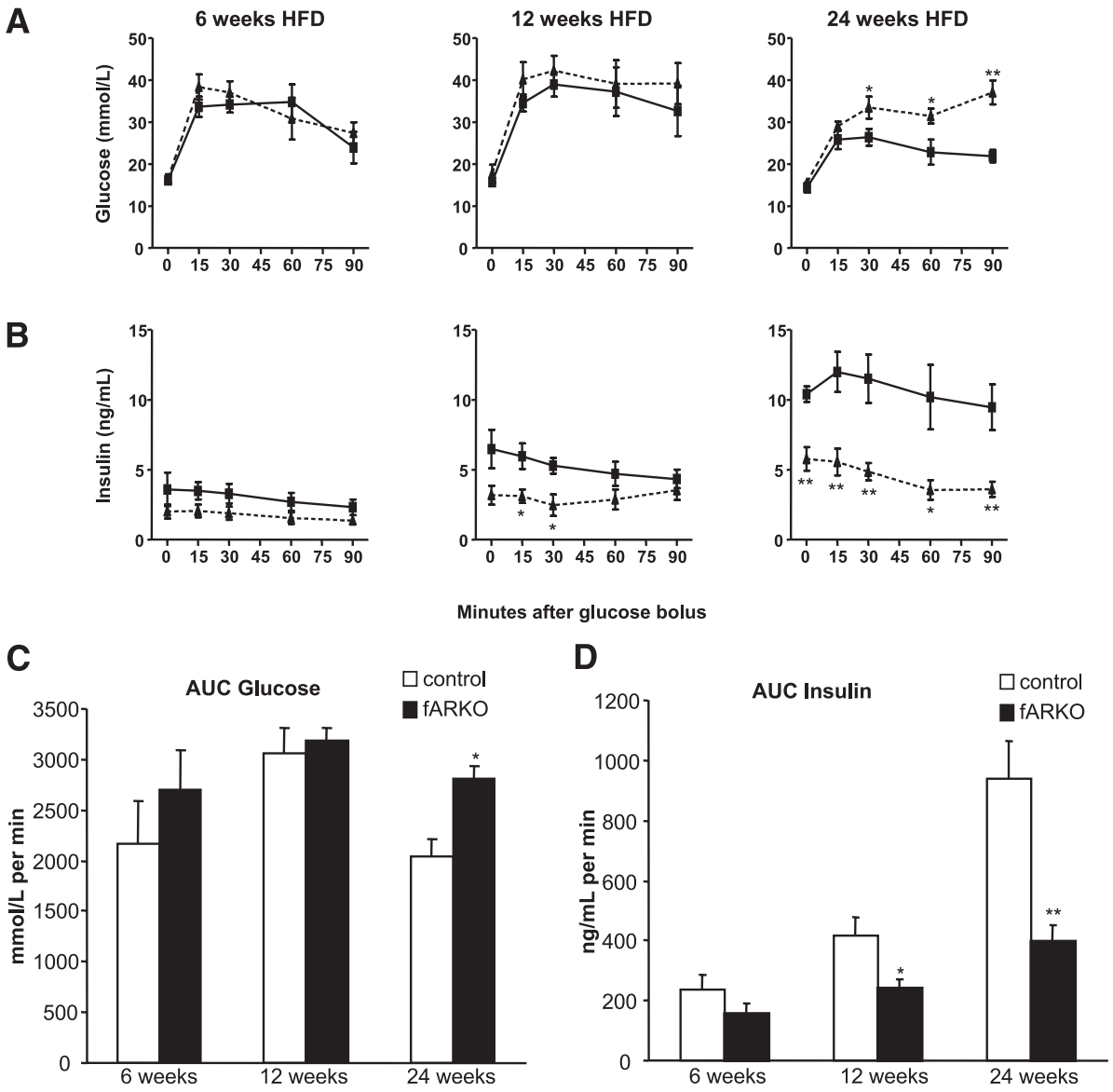

FIG. 6. Effect of HF diet on glucose homeostasis. Plasma glucose (*A* and *C*) and plasma insulin (*B* and *D*) during intraperitoneal GTT of male control and fARKO mice on HF diet for 6, 12, and 24 weeks. Mice were fasted for 6 h before testing. Solid line denotes control mice; broken line denotes fARKO mice. Area under the curve (AUC) for all groups shown for glucose (*C*) and insulin (*D*). Data are mean ± SEM (n = 8–10) for individual time points. *$P < 0.05$, **$P < 0.01$ control vs. fARKO.

downregulation of RBP4 by androgens was confirmed in murine adipocytes in culture.

Testosterone is an important regulator of body composition in males, and there is an inverse relationship between total serum testosterone and the amount of visceral adipose tissue. This is observed in age-related hypogonadism (23), inherited testosterone deficiency (24), and androgen-deprivation therapy during treatment of prostate cancer (25). Several lines of evidence demonstrate that the anti-obesity actions of testosterone are mediated via AR. First, men with genetic androgen resistance linked to CAG repeats in the AR gene, which decreases AR-mediated gene transcription, have an excess of visceral fat (26). Second, male mice lacking AR in all tissues develop late-onset visceral obesity (10,27). Consistent with previous reports in 3-month-old global ARKO mice (27), fARKO mice weighed less than their control littermates. Over the next few weeks, their body weight caught up with that of the control mice; yet in marked contrast with mice with whole-body AR deficiency (10,11), fARKO mice did not spontaneously become obese. This suggests that AR activity in extra-adipose tissues, such as skeletal muscle, contributes to the effect of testosterone on body composition. Of interest, since the Ap2-*cre* "leaks" in CNS and fARKO mice have AR deletion in brain, the current experiment suggests that the spontaneous obesity in global ARKO mice is not attributed to altered androgen action in brain. In keeping with the obesity of androgen resistance being dependent on an interaction between AR signaling in adipose tissue and dietary caloric intake, fARKO mice did accumulate more visceral fat on highly palatable HF feeding. However, detailed metabolic balance studies have yet to be reported to establish the consequences of global or tissue-specific androgen resistance on food intake.

Despite the absence of an increase in body weight and adiposity, fARKO mice on normal diet exhibit impaired insulin sensitivity, as evidenced by hyperinsulinemia both

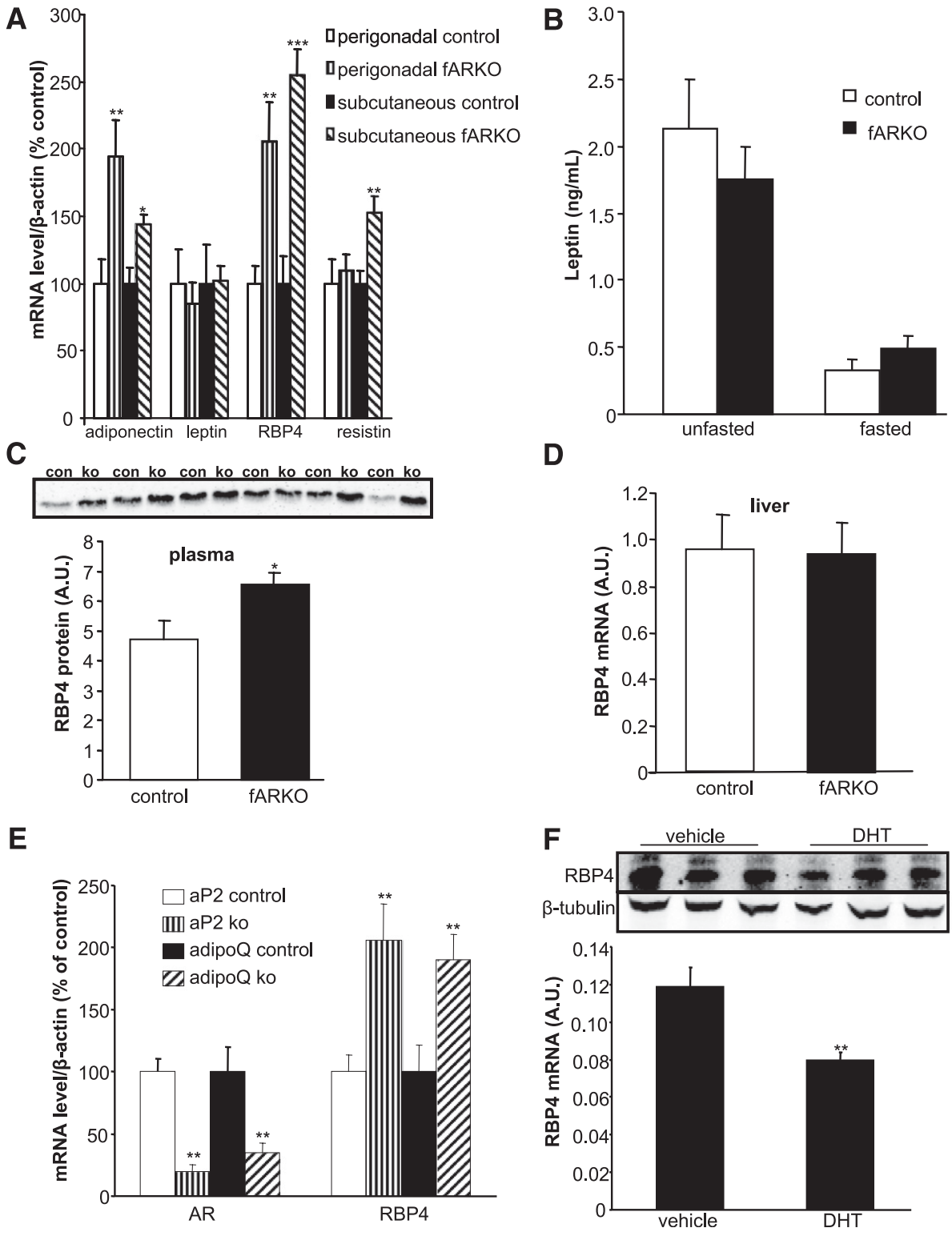

FIG. 7. Increased RBP4 expression in fARKO mice. *A*: Adipokine mRNA expression in perigonadal and subcutaneous fat of 3-month-old fARKO and control mice on standard chow as measured by quantitative PCR. *B*: Circulating fasting (16 h) and fed leptin levels as measured by enzyme-linked immunosorbent assay of 3-month-old control and fARKO plasma. *C*: Circulating RBP4 levels in plasma as measured by Western blot in 3-month-old male control and fARKO mice maintained on standard chow. Con, control; KO, knockout; A.U., arbitrary unit. *D*: Hepatic RBP4 mRNA levels as measured by quantitative PCR in 3-month-old male control and fARKO mice maintained on standard chow. *E*: Adipose mRNA levels for AR and RBP4 as measured by quantitative PCR in perigonadal adipose tissue of 3-month-old male control and fARKO mice generated with aP2-*cre* and adiponectin-*cre* maintained on standard chow. Data are mean ± SEM (n = 8–10). *$P < 0.05$, **$P < 0.01$, ***$P < 0.001$ control vs. KO. *F*: Representative Western blot of RBP4 in 3T3-L1 adipocytes incubated with vehicle (0.01% ethanol) or DHT (100 nmol/L) for 24 h. Data are mean ± SEM. **$P < 0.01$ vs. vehicle treatment.

fasting and during GTTs. This is of similar magnitude to the insulin resistance that occurs at age 20 weeks in nonobese whole-body $AR^{-/y}$ mice (27), suggesting that loss of AR in adipose tissue may directly reduce insulin sensitivity without first increasing body weight or adiposity. However, these findings are in contrast to a previously published adipose-specific ARKO model in which there was no alteration in fasting plasma glucose or insulin at age 20 weeks (12). By assessing glucose tolerance across the life span and with or without the challenge of an HF diet, we demonstrated that insulin resistance is apparent in fARKO mice from age 12 weeks and that insulin deficiency develops with ageing and HF diet. Furthermore, with an HF diet, the adverse metabolic phenotype becomes more severe and fARKO mice develop visceral obesity and hyperglycemia. We therefore sought adipose-derived factors that are likely to explain both insulin resistance and subsequent deficiency.

Among the major models currently proposed for the role of adipose tissue in the pathogenesis of insulin resistance, one proposes that an increase in the release of NEFA from adipose tissue causes insulin resistance, whereas another implicates differences in adipokine levels (28). Fasting NEFA levels were not different between fARKO mice and controls, and NEFA suppression in response to glucose administration was similar in both groups. On the other hand, the expression of several adipokines was altered in fARKO mice. The antidiabetic properties of adiponectin have attracted considerable attention. A number of studies in humans, nonhuman primates, and rodents show that hypoadiponectinemia is a common feature of obesity and insulin resistance (29–31). In contrast, fARKO mice have elevated adiponectin levels. The association between hyperadiponectinemia and insulin resistance has previously been reported in adipocyte-specific Insr knockout (FIRKO) mice (32) and their human counterparts (33) and is consistent with data from global AR-deficient mice (11) and hypogonadal men (34). We infer that testosterone acts via AR in adipose tissue to suppress adiponectin levels in males, but reduced adiponectin is not responsible for insulin resistance in fARKO mice.

Elevated RBP4 levels recently have been reported to be associated with insulin resistance in several insulin-resistant mouse models and in patients with type 2 diabetes (20). In humans, there is a strong association between elevated serum RBP4 concentrations and components of metabolic syndrome, including increased BMI and waist circumference (35). RBP4 expression is higher in visceral versus subcutaneous adipose tissue, regardless of percent body fat, fat distribution, the presence or absence of type 2 diabetes, or adipocyte size; however, the factors regulating this site-specific difference in RBP4 levels remain to be elucidated. In fARKO mice, *Rbp4* mRNA expression is selectively increased in adipose tissue, but not in liver. We are not aware of previous evidence directly relating AR activity with RBP4 in mice, so we explored this interaction in differentiated 3T3-L1 cells in which we showed direct downregulation of RBP4 expression by nonaromatizable androgen. Paradoxically, in humans, plasma RBP4 concentrations have been shown to be higher in males than females (36), RBP4 expression is higher in visceral than subcutaneous adipose tissue (37,38), and higher RBP4 expression has been associated with increased testosterone levels and insulin resistance in women with polycystic ovary syndrome (39); it is likely that regulation of RBP4 expression is complex and influenced not only by androgen signaling but also by other confounding factors. However, consistent with the metabolic phenotype of the fARKO mouse, mice overexpressing RBP4 are hyperinsulinemic and euglycemic and have no differences in NEFA or leptin levels (20). The mechanism by which elevated adipose RBP4 levels induce insulin resistance is unclear; however, evidence suggests that RBP4 may be released from adipocytes and act locally to inhibit Tyr phosphorylation of IRS-1 (40), a molecular defect implicated in human insulin resistance (41). In fARKO mice, insulin-stimulated Tyr phosphorylation of IRS-1 at Tyr residue 612 was significantly reduced. RBP4 may also play an important role in lipid metabolism (42), and most human studies that confirm the association of RBP4 levels with insulin resistance also observe significant associations with lipid levels, in particular with triglyceride, HDL cholesterol, and LDL cholesterol (43–45). Elevated RBP4 therefore provides a plausible mechanism for the metabolic abnormalities observed in fARKO mice.

We conclude that AR signaling in adipose tissue plays a critical role in glucose homeostasis independently of adiposity. Disruption of this signaling can lead to the development of insulin resistance, possibly via the dysregulation of insulin-sensitizing adipokines. Manipulation of AR activity at the level of the adipose tissue may therefore provide a therapeutic target for the treatment of insulin resistance associated with testosterone deficiency in males, while avoiding potential adverse effects in other systems such as prostate gland and hemostasis.

ACKNOWLEDGMENTS

This work was supported by grants from Diabetes UK, the British Heart Foundation, the Medical Research Council, and the Society for Endocrinology.

No potential conflicts of interest relevant to this article were reported.

K.J.M. designed the experiments, researched and analyzed data, and wrote the manuscript. L.B.S. designed the experiments and reviewed and edited the manuscript. N.I.H. researched data (HF model). P.T.K.S., R.A., and B.R.W. contributed to experimental design and reviewed and edited the manuscript. K.J.M. is the guarantor of this work and, as such, had full access to all the data in the study and takes responsibility for the integrity of the data and the accuracy of the data analysis.

Parts of this study were presented in abstract form at the 93rd Annual Meeting and Expo of The Endocrine Society, San Diego, California, 19–22 June 2010; the British Endocrine Society Meeting, Manchester, U.K., 15–18 March 2010; and the Diabetes UK Annual Professional Conference, Liverpool, U.K., 3–5 March 2010.

The authors are grateful to Karel de Gendt and Guido Verhoeven (Catholic University of Leuven, Leuven, Belgium) for providing the AR^{flox} mice and to Mirela Delibegovic (University of Aberdeen, Scotland) for providing adiponectin-*cre* mice. The authors thank Nimesh Mody (University of Aberdeen) for RBP4 antibody and the staff of the Biomedical Research Facility, University of Edinburgh, for technical assistance.

REFERENCES

1. Kapoor D, Malkin CJ, Channer KS, Jones TH. Androgens, insulin resistance and vascular disease in men. Clin Endocrinol (Oxf) 2005;63:239–250
2. Grossmann M, Gianatti EJ, Zajac JD. Testosterone and type 2 diabetes. Curr Opin Endocrinol Diabetes Obes 2010;17:247–256
3. Barrett-Connor E. Lower endogenous androgen levels and dyslipidmia in men with non-insulin-dependent diabetes mellitus. Ann Intern Med 1992; 117:807–811

4. Kapoor D, Goodwin E, Channer KS, Jones TH. Testosterone replacement therapy improves insulin resistance, glycaemic control, visceral adiposity and hypercholesterolaemia in hypogonadal men with type 2 diabetes. Eur J Endocrinol 2006;154:899–906
5. Hamilton EJ, Gianatti E, Strauss BJ, et al. Increase in visceral and subcutaneous abdominal fat in men with prostate cancer treated with androgen deprivation therapy. Clin Endocrinol (Oxf) 2011;74:377–383
6. Jones TH. Testosterone deficiency: a risk factor for cardiovascular disease? Trends Endocrinol Metab 2010;21:496–503
7. Joyner J, Hutley L, Cameron D. Intrinsic regional differences in androgen receptors and dihydrotestosterone metabolism in human preadipocytes. Horm Metab Res 2002;34:223–228
8. Singh R, Artaza JN, Taylor WE, et al. Testosterone inhibits adipogenic differentiation in 3T3-L1 cells: nuclear translocation of androgen receptor complex with beta-catenin and T-cell factor 4 may bypass canonical Wnt signaling to down-regulate adipogenic transcription factors. Endocrinology 2006;147:141–154
9. Movérare-Skrtic S, Venken K, Andersson N, et al. Dihydrotestosterone treatment results in obesity and altered lipid metabolism in orchidectomized mice. Obesity (Silver Spring) 2006;14:662–672
10. Sato T, Matsumoto T, Yamada T, Watanabe T, Kawano H, Kato S. Late onset of obesity in male androgen receptor-deficient (AR KO) mice. Biochem Biophys Res Commun 2003;300:167–171
11. Fan WQ, Yanase T, Nomura M, et al. Androgen receptor null male mice develop late-onset obesity caused by decreased energy expenditure and lipolytic activity but show normal insulin sensitivity with high adiponectin secretion. Diabetes 2005;54:1000–1008
12. Yu IC, Lin HY, Liu NC, et al. Hyperleptinemia without obesity in male mice lacking androgen receptor in adipose tissue. Endocrinology 2008;149: 2361–2368
13. Lin HY, Yu IC, Wang RS, et al. Increased hepatic steatosis and insulin resistance in mice lacking hepatic androgen receptor. Hepatology 2008;47: 1924–1935
14. Eguchi J, Wang X, Yu ST, et al. Transcriptional control of adipose lipid handling by IRF4. Cell Metab 2011;13:249–259
15. De Gendt K, Swinnen JV, Saunders PTK, et al. A Sertoli cell-selective knockout of the androgen receptor causes spermatogenic arrest in meiosis. Proc Natl Acad Sci U S A 2004;101:1327–1332
16. Welsh M, Saunders PTK, Atanassova N, Sharpe RM, Smith LB. Androgen action via testicular peritubular myoid cells is essential for male fertility. FASEB J 2009;23:4218–4230
17. Morton NM, Holmes MC, Fiévet C, et al. Improved lipid and lipoprotein profile, hepatic insulin sensitivity, and glucose tolerance in 11beta-hydroxysteroid dehydrogenase type 1 null mice. J Biol Chem 2001;276: 41293–41300
18. Winzell MS, Ahrén B. The high-fat diet-fed mouse: a model for studying mechanisms and treatment of impaired glucose tolerance and type 2 diabetes. Diabetes 2004;53(Suppl. 3):S215–S219
19. Corker CS, Davidson DW. A radioimmunoassay for testosterone in various biological fluids without chromatography. J Steroid Biochem 1978;9:373–374
20. Yang Q, Graham TE, Mody N, et al. Serum retinol binding protein 4 contributes to insulin resistance in obesity and type 2 diabetes. Nature 2005; 436:356–362
21. De Sousa Peixoto RA, Turban S, Battle JH, Chapman KE, Seckl JR, Morton NM. Preadipocyte 11beta-hydroxysteroid dehydrogenase type 1 is a ketoreductase and contributes to diet-induced visceral obesity in vivo. Endocrinology 2008;149:1861–1868
22. McInnes KJ, Corbould A, Simpson ER, Jones ME. Regulation of adenosine 5′, monophosphate-activated protein kinase and lipogenesis by androgens contributes to visceral obesity in an estrogen-deficient state. Endocrinology 2006;147:5907–5913
23. Zitzmann M, Faber S, Nieschlag E. Association of specific symptoms and metabolic risks with serum testosterone in older men. J Clin Endocrinol Metab 2006;91:4335–4343
24. Bojesen A, Kristensen K, Birkebaek NH, et al. The metabolic syndrome is frequent in Klinefelter's syndrome and is associated with abdominal obesity and hypogonadism. Diabetes Care 2006;29:1591–1598
25. Basaria S, Muller DC, Carducci MA, Egan J, Dobs AS. Hyperglycemia and insulin resistance in men with prostate carcinoma who receive androgen-deprivation therapy. Cancer 2006;106:581–588
26. Zitzmann M, Gromoll J, von Eckardstein A, Nieschlag E. The CAG repeat polymorphism in the androgen receptor gene modulates body fat mass and serum concentrations of leptin and insulin in men. Diabetologia 2003; 46:31–39
27. Lin HY, Xu QQ, Yeh SY, Wang RS, Sparks JD, Chang CS. Insulin and leptin resistance with hyperleptinemia in mice lacking androgen receptor. Diabetes 2005;54:1717–1725
28. Kobayashi K. Adipokines: therapeutic targets for metabolic syndrome. Curr Drug Targets 2005;6:525–529
29. Hotta K, Funahashi T, Bodkin NL, et al. Circulating concentrations of the adipocyte protein adiponectin are decreased in parallel with reduced insulin sensitivity during the progression to type 2 diabetes in rhesus monkeys. Diabetes 2001;50:1126–1133
30. Yatagai T, Nagasaka S, Taniguchi A, et al. Hypoadiponectinemia is associated with visceral fat accumulation and insulin resistance in Japanese men with type 2 diabetes mellitus. Metabolism 2003;52:1274–1278
31. Hu E, Liang P, Spiegelman BM. AdipoQ is a novel adipose-specific gene dysregulated in obesity. J Biol Chem 1996;271:10697–10703
32. Blüher M, Michael MD, Peroni OD, et al. Adipose tissue selective insulin receptor knockout protects against obesity and obesity-related glucose intolerance. Dev Cell 2002;3:25–38
33. Semple RK, Soos MA, Luan J, et al. Elevated plasma adiponectin in humans with genetically defective insulin receptors. J Clin Endocrinol Metab 2006;91:3219–3223
34. Lanfranco F, Zitzmann M, Simoni M, Nieschlag E. Serum adiponectin levels in hypogonadal males: influence of testosterone replacement therapy. Clin Endocrinol (Oxf) 2004;60:500–507
35. Graham TE, Yang Q, Mody N, et al. Serum retinol binding protein (RBP4) is a novel adipocyte-secreted protein elevated in obesity and type 2 diabetes that contributes to insulin resistance. Diabetes 2005; 54:A5
36. Cho YM, Youn BS, Lee H, et al. Plasma retinol-binding protein-4 concentrations are elevated in human subjects with impaired glucose tolerance and type 2 diabetes. Diabetes Care 2006;29:2457–2461
37. Klöting N, Graham TE, Berndt J, et al. Serum retinol-binding protein is more highly expressed in visceral than in subcutaneous adipose tissue and is a marker of intra-abdominal fat mass. Cell Metab 2007;6: 79–87
38. Graham TE, Klöting N, Berndt J, et al. Serum retinal binding protein (RBP4) levels predict intraabdominal fat mass. Diabetes 2007;56:A365
39. Tan BK, Chen J, Lehnert H, Kennedy R, Randeva HS. Raised serum, adipocyte, and adipose tissue retinol-binding protein 4 in overweight women with polycystic ovary syndrome: effects of gonadal and adrenal steroids. J Clin Endocrinol Metab 2007;92:2764–2772
40. Ost A, Danielsson A, Lidén M, Eriksson U, Nystrom FH, Strålfors P. Retinol-binding protein-4 attenuates insulin-induced phosphorylation of IRS1 and ERK1/2 in primary human adipocytes. FASEB J 2007;21:3696–3704
41. Danielsson A, Ost A, Lystedt E, et al. Insulin resistance in human adipocytes occurs downstream of IRS1 after surgical cell isolation but at the level of phosphorylation of IRS1 in type 2 diabetes. FEBS J 2005;272:141–151
42. Wu Y, Li HX, Loos RJF, et al. RBP4 variants are significantly associated with plasma RBP4 levels and hypertriglyceridemia risk in Chinese Hans. J Lipid Res 2009;50:1479–1486
43. Graham TE, Yang Q, Blüher M, et al. Retinol-binding protein 4 and insulin resistance in lean, obese, and diabetic subjects. N Engl J Med 2006;354: 2552–2563
44. Takebayashi K, Suetsugu M, Wakabayashi S, Aso Y, Inukai T. Retinol binding protein-4 levels and clinical features of type 2 diabetes patients. J Clin Endocrinol Metab 2007;92:2712–2719
45. Lee DC, Lee JW, Im JA. Association of serum retinol binding protein 4 and insulin resistance in apparently healthy adolescents. Metabolism 2007;56: 327–331